UCRL-CONF-211065

LAWRENCE
LIVERMORE
NATIONAL
LABORATORY

The development of a ductility-based aging model for low temperature aged U-6Nb alloy

Bob Bridges

April 5, 2005

The 26th Compatibility, Aging, and Stockpile Stewardship Conference
Aiken, SC, United States
April 26, 2005 through April 28, 2005

The Development of a Ductility-Based Aging Model for Low Temperature Aged U-6Nb Alloy

T.C. Sun[1] and Bob Bridges[2]
[1]Lawrence Livermore National Laboratory, [2]Y-12 National Security Complex

Abstract

This study focuses on the ductility evaluation of low-temperature (100° and 200°C) aged U-6Nb alloy. The objective is to develop a ductility-based aging model to improve lifetime prediction for weapon components in the stockpile environment.

Literature review shows that the work hardening n-value and the strain-rate hardening m-value are the two most important metallurgical factors for the uniform and the post-uniform (necking) ductility control, respectively. Unfortunately, both n and m values of the U-6Nb alloy are lacking.

The study shows that the total ductility of U-6Nb is dominated by the uniform ductility, which deteriorates in both 100°C and 200°C aging. Further analysis shows that the uniform ductility correlates well with the work hardening n-value of the later stage deformation in which dislocation-slip is the mechanism. The kinetics of the loss of uniform ductility and the associated reduction in work-hardening n-value in low temperature aging will be used for the development of a ductility-based aging model.

The necking ductility appears to be a minor but significant factor in the total ductility of U-6Nb. It does not show a clear trend due to large data scatter. The uncertain nature of necking failure may always hinder a reliable measurement of necking ductility. Consequently, a precise measurement of strain-rate hardening m-value could be a viable alternative to model the metallurgical contribution to the necking ductility. The conventional strain rate step-change method and the ABI (Automated-Ball-Indentation) test both show promising result in m-value measurement.

Introduction

The kinetics of the strength increase of U-6Nb in low temperature aging has been well studied. But the associated loss of ductility was less quantitatively analyzed. There are two hardening mechanisms in typical tensile test; the work hardening described by the work hardening exponent (n-value) and the strain-rate hardening described by the strain-rate sensitivity (m-value). A simplified constitutive equation is given by:

$$\sigma = K \varepsilon^n \acute{\varepsilon}^m$$

where σ is the true stress, ε is the true strain, and $\acute{\varepsilon}$ is the strain rate.

It is well documented that the uniform ductility is related to the work hardening n-value, while the necking ductility is related to the strain-rate hardening m-value. This can be best demonstrated in Fig. 1. Therefore, it is a reasonable goal to develop a precise and ductility-based aging model for low-temperature aged U-6Nb through analyzing n and m values as functions of aging temperature and aging time.

The U-6Nb alloy has a very complicated deformation behavior, and does not follow a single constitutive equation for n-value calculation for its entire stress-strain curve. It starts to deform by twinning, followed by de-twinning, and finally fractures by the dislocation-slip mechanism. Different work hardening n-values are expected for different deformation mechanisms.

The current study demonstrates that the new ABI (Automated-Ball-Indentation) test at Y-12 and the conventional strain rate step-change method are both viable tools for the m-value measurement. The advantages of fast, low-cost, and non-destructive nature of ABI test deserves further evaluation for ESC.

Material and Test Methods

Materials: A 14-year-old Y-12 produced stockpile return component was used in the study. The component has an initial water-quenched condition.

Aging Process: 200°C for 2, 8, 24, and 96 hours
100°C for 30 days and 77 days

Results and Discussions

On Stress-Strain Curve

A typical engineering stress-strain curve of U-6Nb is shown in Fig.2. The marked maximum engineering stress defines the uniform elongation and the necking elongation. The curve also shows a complicated deformation behavior which includes the twinning in the first 3% strain, the de-twining between 3 to 6% strain, a diffuse peak between 6-10% strain, and the final work-hardening by the dislocation-slip mechanism beyond 10% strain.

The early stage twinning-related deformation shows a much higher work hardening rate (a rapid increase in strength) than that of the later stage deformation by dislocation-slip. Aging at 200°C affects the work-hardening behavior of U-6Nb. It increases the work hardening in twinning, while reduces the work hardening in the subsequent dislocation-slip deformation, Fig. 3. All the twinning deformation ceases at around 6% strain regardless of the aging conditions. The extent of the uniform ductility is expected to be controlled by the work-hardening capacity during the later dislocation-slip deformation.

On Strength and Ductility

200℃ aging

U-6Nb shows a sharp increase in the yield strength (from 27 ksi to 100 ksi) and a moderate increase in the ultimate tensile strength (from 123 ksi to136 ksi) when aged at 200°C, Fig. 4.

The total elongation (uniform + necking) shows a decreasing trend but with substantial data scatter. The scatter is primarily from the necking component. The uniform elongation, which accounts for 70-80% of the total ductility, is a fairly reliable property and shows a clear decreasing trend, Fig. 5. The necking elongation is a minor but significant component. Due to the large data scatter, necking ductility does not show a clear trend.

100℃ aging

Figure 6 shows moderate but clear increase in yield strength and decrease in ductility when aged at 100°C for up to 77 days. Again, the uniform ductility is a dominant factor with a decreasing trend, while the necking ductility show large scatter.

On Work-Hardening n-value and Uniform Ductility

U-6Nb is deformed by twinning during the first 6% strain followed by a dislocation-slip mechanism to the final fracture at around 25% strain. A detailed analysis on the true stress–true strain curves confirms that there is a single work hardening n-value in the dislocation-slip region up to the uniform ductility limit. And this later stage n-value correlates well with the uniform ductility limit of U-6Nb, Fig. 7.

The good correlation between the uniform ductility limit and the later stage n-value covers a wide range of metal conditions such as water-quenched, naturally aged, low-temperature artificially aged, and mistakenly high-temperature aged conditions.

On Strain-Rate Hardening m-value and necking ductility

The strain-rate hardening m-value is the most significant metallurgical properties for the necking ductility control. Figure 8 shows the strain-rate step-change test on U-6Nb and Ta. The benefit of higher m-value of Ta (0.027 vs. 0.008 of U-6Nb) on larger necking ductility is demonstrated in Fig. 9.

On ABI Test

Figure 10 and Figure 11 show the ABI's true stress-true strain curves of 200^{o}C aged U-6Nb under low (0.0001 in./sec) and high (0.1 in./sec) strain rates test conditions. It demonstrates the excellent capability of ABI for metal strength and strain rate sensitivity evaluation.

Conclusions

1. We developed the metallurgical principles of ductility control for U-6Nb.
2. The total ductility of U-6Nb is dominated by the uniform ductility, and the necking ductility is a minor but significant factor.
3. The uniform ductility shows a clear decreasing trend in both 100° and 200°C aging. The kinetics of the loss of uniform ductility and the associated reduction in work-hardening n-value has been developed for modeling work.
4. The necking ductility evaluation is inconclusive due to the large data scatter. Measurement of the strain-rate hardening m-value is a viable alternative to model the necking ductility.
5. The ABI test shows good potential as a cost-effective tool to evaluate the work hardening and the strain-rate hardening behaviors of U-6Nb.

This work was performed under the auspices of the U.S. Department of Energy by University of California, Lawrence Livermore National Laboratory under Contract W-7405-Eng-48, and by BWXT Y-12, L.L.C. under Contract DE-AC05-00OR22800.

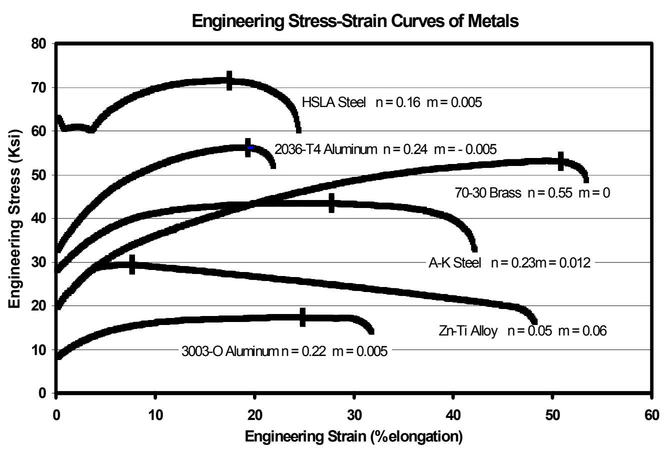

Figure 1: Engineering stress-strain curves of various metals showing good correlations of n and m values on uniform and necking ductility.

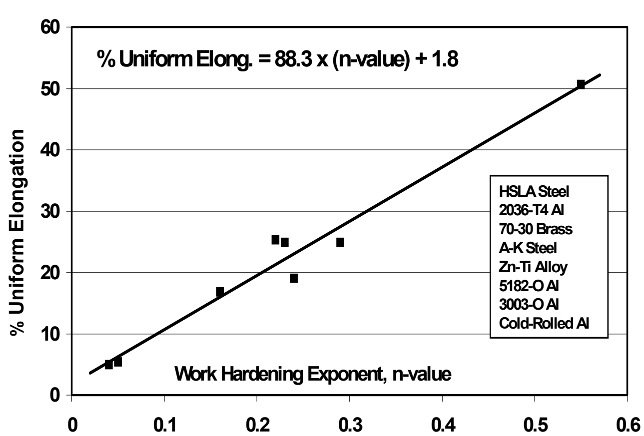

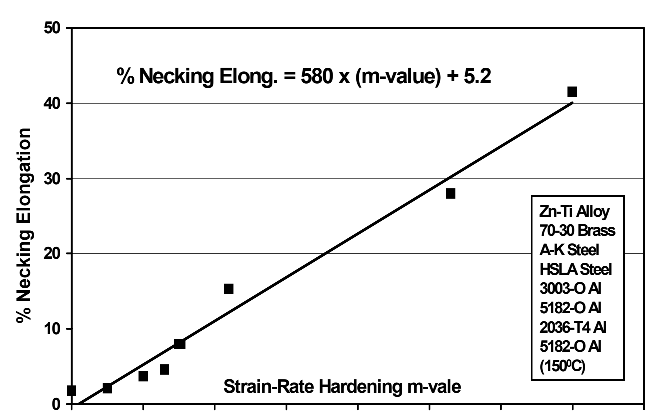

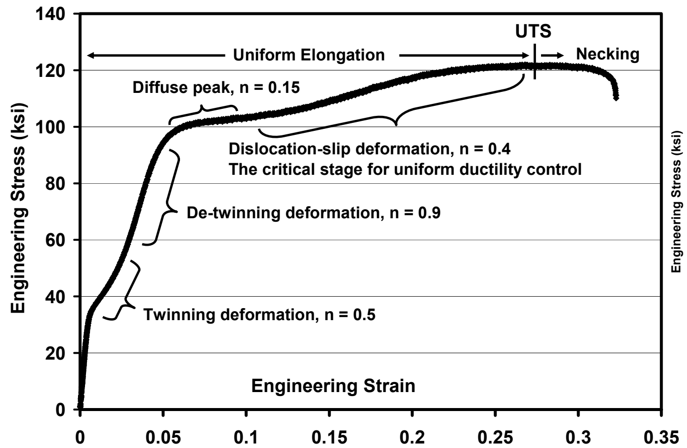

Figure 2: Engineering stress-strain curve of U-6Nb showing different work hardening regions.

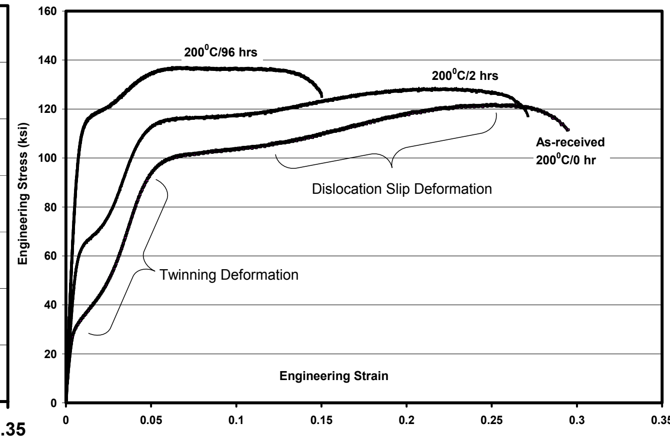

Figure 3: Engineering stress-strain curves of U-6Nb showing the work hardening (slope of the curves) increases in early twinning and decreases in later dislocation-slip deformation by 200°C aging.

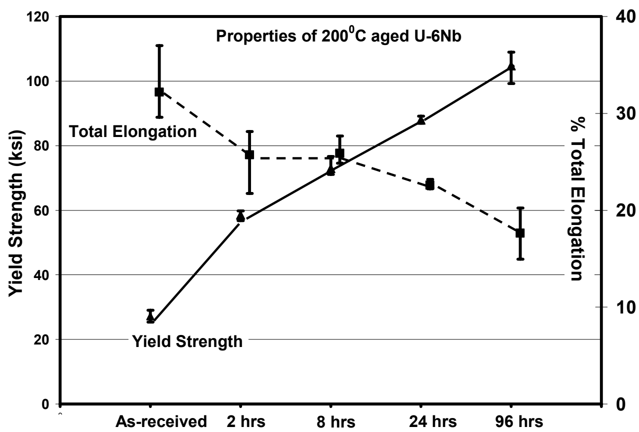

Figure 4: Properties of 200^0C aged U-6Nb. Note the large scatter in total elongation data.

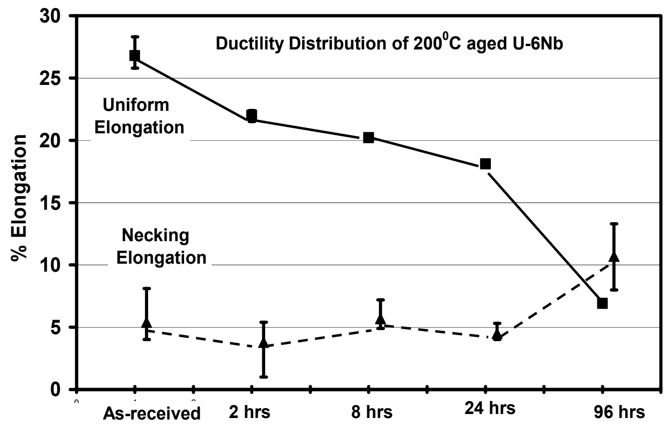

Figure 5: Ductility distribution showing dominant uniform elongation with a decreasing trend in aging, while necking ductility shows large scatter.

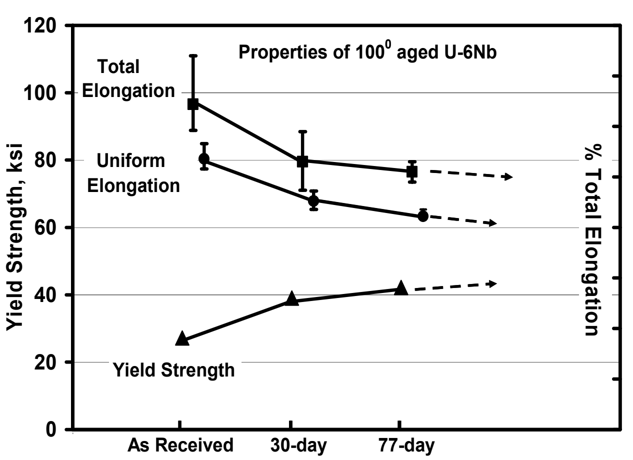

Figure 6: Properties of 100^0C aged U-6Nb showing moderate strength increase and ductility decrease.

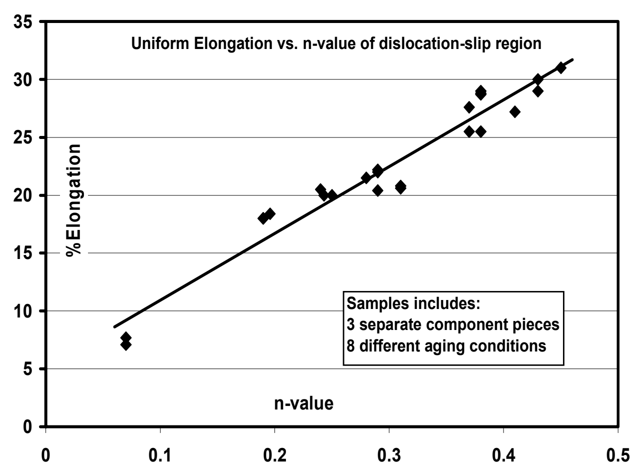

Figure 7: Excellent correlation between the n-value of dislocation–slip region and the uniform elongation for a wide range of aging conditions of U-6Nb.

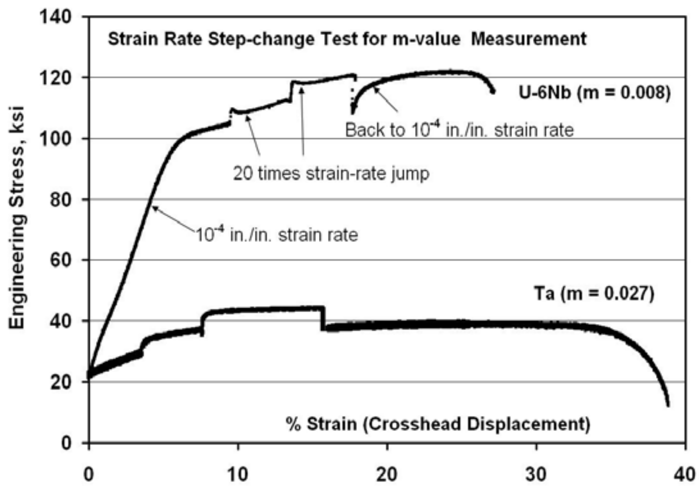

Figure 8: Strain rate step-change tests showing a much larger m-value of Ta than that of U-6Nb.

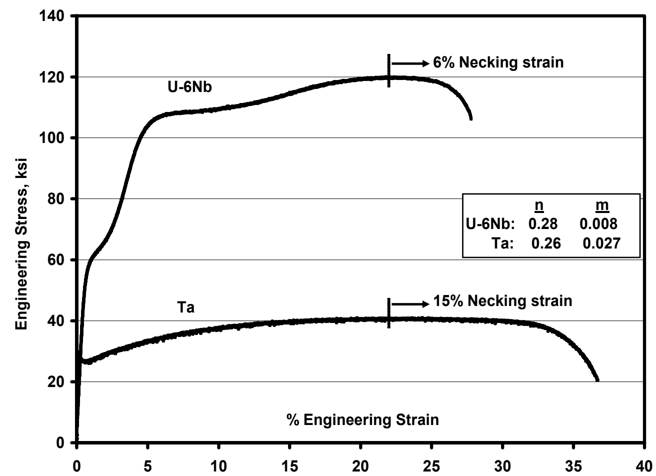

Figure 9: Engineering stress-strain curves of U-6Nb and Ta showing the benefit of large m-value of Ta on necking ductility.

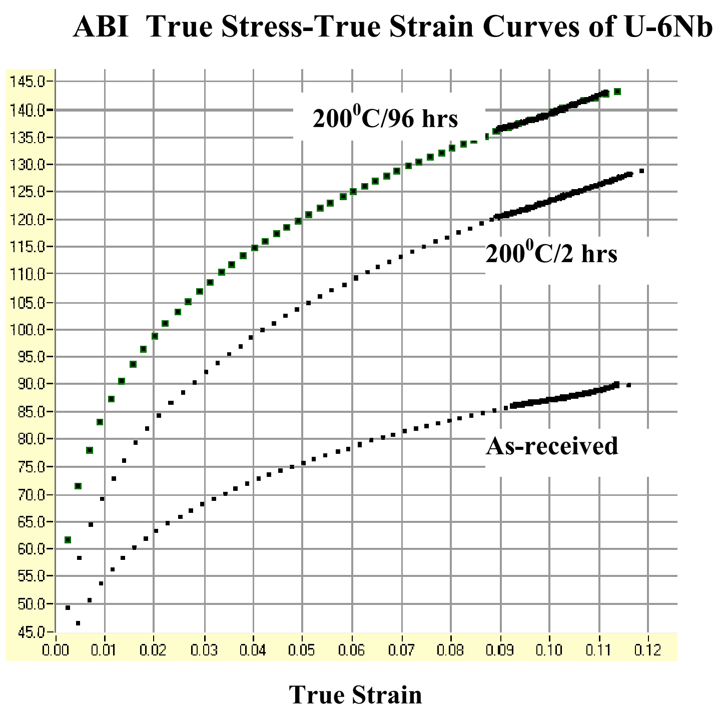

Figure 10: ABI data showing strong age-hardening behaviors in 200^0C aging.

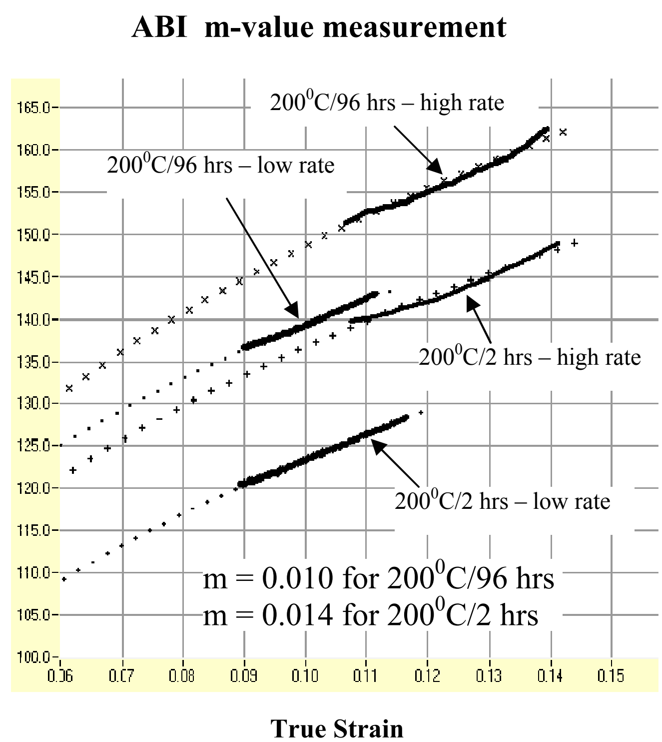

Figure 11: ABI data showing strain-rate hardening behaviors of 200^0C aged U-6Nb (0.0001 in./sec low rate vs. 0.1 in./sec high rate).